

# Torque Ripple Measurements of a Special Switched Reluctance Motor

S. I. Nabeta<sup>1</sup>, I. E. Chabu<sup>1</sup>, L. Lebensztajn<sup>1</sup>, J. R. Cardoso<sup>1</sup>,  
M. C. Costa<sup>2</sup>, K. Hameyer<sup>3</sup>, D. A. P. Corrêa<sup>4</sup>, W. M. da Silva<sup>4</sup>

<sup>1</sup>LMAG-PEA-EPUSP, Laboratório de Eletromagnetismo Aplicado, 05508-900 – São Paulo, Brazil

<sup>2</sup>IPT-SP, Instituto de Pesquisas Tecnológicas, 05508-900 – São Paulo, Brazil

<sup>3</sup>IEM, Institut für Elektrische Maschinen, RWTH, D-52506, Aachen, Germany

<sup>4</sup>CTM-SP, Centro Tecnológico da Marinha em São Paulo, 05508-900 – São Paulo, Brazil

e-mail: [dapcorrea@yahoo.com.br](mailto:dapcorrea@yahoo.com.br) and [wmarinho@usp.br](mailto:wmarinho@usp.br)

**Abstract** – This paper presents an indirect method of torque ripple measurement, considering a special Switched Reluctance Motor – SRM, operating at nominal speed and torque conditions. The SRM under test has 4:2 pole, two phases, fractional power, and it will be used with high-speed manual machine tools. The measured data refer to two different rotors, an original and an optimized one. The experimental results were compared with simulated and calculated values, validating the theoretical base.

**Keywords:** SRM - Switched reluctance motor, tests, vibration.

## I – INTRODUCTION

Switched Reluctance Motors are in general a good choice for several industry applications, due to their mechanical and thermal robustness. They are easily manufactured and represent a low production cost. However, they show two disadvantages: its torque ripple and acoustic noise.

The switched power supply and the control strategy applied to these motors generate vibrations, which could be classified into two types: mechanical and magnetic [1] [2]. The effects of these vibrations could add up and, as a consequence, increase the vibrations and acoustic noise.

The main problem to realize bench tests with these kinds of motors is to measure the torque ripple, which requires a special sensor coupled to the motor shaft. These sensors have some technical constraints because they are accurate for only for a narrow range of speed and torque and they are also expensive.

Thus, in this paper, an alternative and indirect method of measurement of the torque ripple is presented, using the vibration data. The measured data refer to two different rotors, the original and the optimized one, and the results were compared with the calculated values, obtained from a numeric approach using the Finite Element Method together with an optimization algorithm, which includes a Kriging model, and the Simulated Annealing method - SA.

## II – SWITCHED RELUCTANCE MOTOR CHARACTERISTICS

Table I presents the SRM main characteristics:

TABLE I. SRM MAIN CHARACTERISTICS

Parameter	Value
Number of Phases	2
Stator / Rotor Poles	4 / 2
Nominal Power	½ HP
Nominal Current	1.7 Amps rms
Nominal Speed	6000 rpm
Nominal Torque	0.28 N.m

The SRM has specially designed rotor poles with an original geometry, in order to improve the torque characteristics, which ensures the starting torque in a defined direction at any rotor position [3], [4], [5], [6]. The rotor poles present a geometric asymmetry, which consists of one region with a small uniform air-gap and another with a variable air-gap, which increases towards the quadrature axis.

The complete motor structure is depicted in Fig. 1(a), while the pole details are shown in Fig. 1(b). The general geometric characteristics of this SRM are summarized in table II.

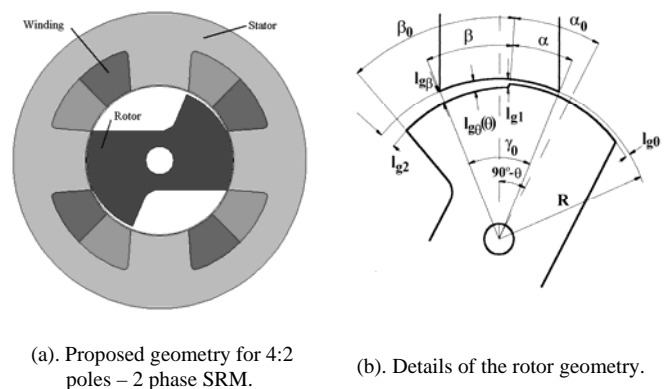


Fig.1 The Motor Geometry

TABLE II. GEOMETRIC CHARACTERISTICS OF THE SRM

Characteristic	Value
Stator outer diameter	90 mm
Stator yoke thickness	10 mm
Rotor diameter	$2R = 45$ mm
Core length	$L_c = 35$ mm
Stator pole arc	$\gamma_0 = 45^\circ$
Rotor pole arc	$2\alpha_0 = 45^\circ$
Main air-gap thickness	$l_{g0} = 0.3$ mm

### III – THE POWER DRIVE AND CONTROL CIRCUIT

In order to simplify the power drive topology, it was used a conventional asymmetric converter with only four power MOSFET's switches (S1, S2 S3 and S4), as shown in Fig. 2(a) e 2(b) [7] [8]. The SRM rotor position detection is based on an optical sensor, located in the motor stator, and it allows adjusting the commutation angles, since the turn-on and turn-off firing angles interval cannot be altered.

A hysteresis (bang-bang) circuit controls the phase currents. When the phase current limit is not reached, the motor drive works in a single pulse operation mode. To accomplish the vibration experiment, it was adopted a single pulse operation mode to avoid possible PWM contributions in the vibrations results.

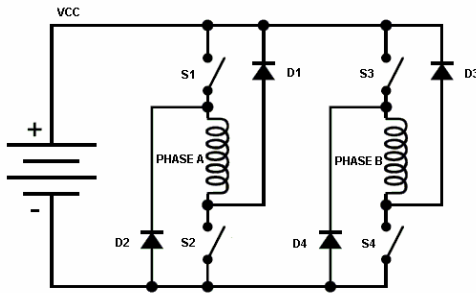


Fig. 2 (a). Conventional Asymmetric Converter

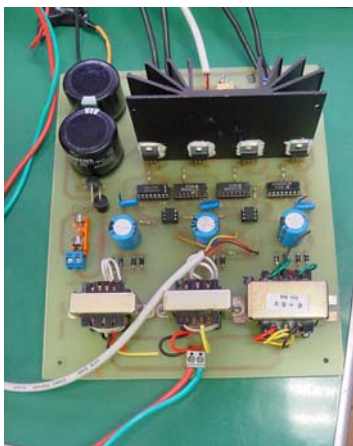


Fig. 2 (b). Power drive prototype

### IV – THE ROTOR OPTIMIZATION PROCEDURES

The torque ripple was minimized by optimizing the SRM rotor using Finite Element Method (FEM) and a numerical approach, based on the application of Simulated Annealing (SA) and Kriging Method [3] [4] [5] [6].

In most cases, the minimization of the torque ripple implies in degradation of other important features, such as: the starting and the average torques. Optimization techniques were applied, where the torque ripple was minimized, submitted to two constraints: a minimum starting torque and a minimum average torque [4].

In order to reach this objective, the geometric parameters of the rotor  $\beta_0$ ,  $l_{g1}$  and  $l_{g2}$  (Fig. 1 (b)) were chosen as the most significant for the optimization process [5] [6].

The variation domain of each geometric parameter to be optimized was defined following the values presented in Table III.

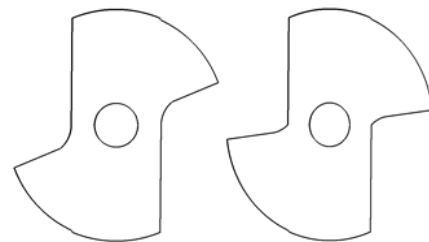
TABLE III. PARAMETERS VARIATION DOMAIN

Parameter	Reference Value	Minimum Value	Maximum Value
$\beta_0$	$45^\circ$	$30^\circ$	$60^\circ$
$l_{g1}$	0.6 mm	0.4 mm	0.6 mm
$l_{g2}$	1.2 mm	0.6 mm	1.8 mm

From the Finite Element Method (FEM), it was possible to reach the optimization objectives replacing the objective function for an approximated function, allowing an important reduction in the number of simulations.

After application a SA and the Kriging model, the values obtained for the optimized parameters were:  $\beta_0 = 60^\circ$ ,  $l_{g1} = 0.5$  mm and  $l_{g2} = 1.0$  mm. So, the rotor with new dimensions was named as optimized.

The Fig. 3 (a) (b) and Fig. 4 (a) (b) show the stator and the rotor geometry before and after the optimization respectively.



(a) Before optimization (b) After optimization  
Fig. 3. Rotor Geometry

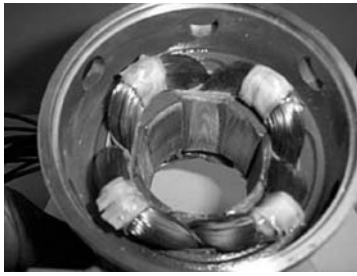


Fig. 4 (a) SRM Stator

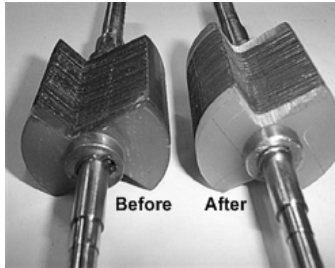


Fig. 4. (b) SRM rotors prototypes

## V – VIBRATION ANALYSIS

There are many variables involved with SRM vibration process, such as, uniformity of the materials, lamination stacking, mounting conditions, stiffness and mass of the windings. It is extremely difficult to introduce these variables in the numerical computational model of the SRM. Many parameters should be evaluated considering manufacturing variations and difficulties in calculating, for example, the winding stiffness [1]. Furthermore, there are some parameters, which should be obtained by experimental tests, for instance, the damping coefficient.

There are several methods to measure motor vibrations [1] [2]. The practical tests vibrations could be performed with a locked rotor (static) or at nominal speed. In static tests it is used, for example, the hammer or the shaker to stimulate or excite the vibrations in the motor, whereas in the dynamic tests, the own motor phase current excites the motor vibrations.

The vibration analysis is well known as modal analysis, which is divided in four basic stages: excitation, data acquisition, signals processing and parameters extraction [1].

The vibration measures can be accomplished in time or frequency domain [1] [2]. The time domain analysis can reveal the connection among the acoustic noise, the stator vibrations, shape, and timing of the applied voltage and the current in the motor windings, while the frequency domain, is used to evaluate the spectrum dominant components of noise and vibration [2].

## VI – EXPERIMENTAL TESTS

The vibration experimental tests were accomplished in the frequency domain, to evaluate the frequency spectrum dominant components present in the torque ripple signal. The SR motor was tested with the two rotors available, the original and the optimized one, to validate the optimization process implemented.

The SRM test bench setup is shown in Fig. 5 and presents all electronic and electromechanical instruments/equipments necessary to carry out the tests.

The SRM torque ripple measurements were carried out with the motor running near the nominal speed and torque values, i.e., 6000 rpm and 0,28 N.m. The load torque was provided by an electromagnetic brake (Foucault method), acting in an inertia disc coupled to the SRM rotor shaft. The SRM shaft torque was measured using a Teldix Load cell coupled to a Teldix Torque Measure Instrument.

The two rotors were tested at the same commutation angle condition. The commutation angle was kept fixed at  $45^\circ$  advanced to the stator/rotor alignment.

The motor stator was connected to a piezoelectric accelerometer sensor from Brüel & Kjaer. The accelerometer sensor signal was applied to the amplifier and conditioning module - Brüel & Kjaer Charge Amplifier. The Charge Amplifier parameters as gain, unit, work range, and off-set were adjusted, in order to convert the accelerometer sensor signal from  $\text{m/s}^2$  to a proportional voltage signal. The output voltage signal from the Charge Amplifier was applied to the Dynamic Signal Analyzer to accomplish the signal treatment in the frequency domain. Using a Fast Fourier Transform – FFT method, the Dynamic Signal Analyzer converted the Charge Amplifier output voltage signal, from time domain to frequency domain. The Dynamic Signal Analyzer was set up to Hanning window mode and anti-aliasing internal filters. The Dynamic Signal Analyzer was also kept in auto-scale voltage level, and the frequency accuracy was defined as 0.125 Hz.

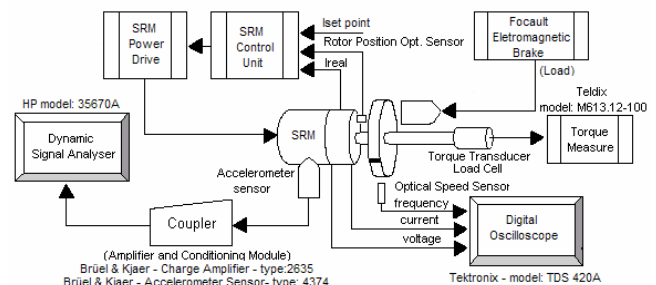


Fig. 5. SRM Test Bench setup

## VII– RESULTS

### A. Theoretical results

Using the Finite Element Method (FEM) simulations, considering nonlinear ferromagnetic material, were carried out. Only one of the phases motor was fed with the rated magnetomotive force in the angular range from  $0^\circ$  to  $90^\circ$ . Thus, it was obtained the curve of the Torque vs. Angular Position before and after the optimization process as shown in Fig. 6.

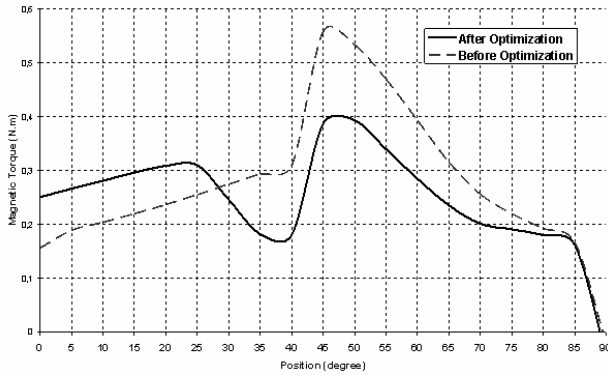


Fig. 6. Magnetic torque developed before and after optimization.

The ripple torque is defined as the difference between the maximum and the minimum values from 0° to 90° region. Considering the original design as the reference, the optimized prototype presents a 44% smaller torque ripple as shown in Fig. 6

### B. Experimental results

It is worth observing that the torque ripple was obtained indirectly, i.e., it was not obtained absolute values of vibration, but relative ones which are depicted in Fig. 7. To fit the two vibration results curves in the same graphic frame, the waveform data from the Dynamic Analyzer were treated using the Matlab [9] software.

The comparison between the vibration curves from the original and the optimized prototypes running at about 6000 rpm is presented in Fig. 7, where it can be noticed that the optimized prototype presents a 72.65% torque ripple reduction. Note that at the nominal rotor speed of 100 Hz or 6000 rpm, the main component of the torque ripple frequency is 400 Hz (four times the rotor frequency).

This significant vibration reduction using the optimized rotor, confirms the numerical results and the torque characteristics improvement proposed in [4] [5] [6].

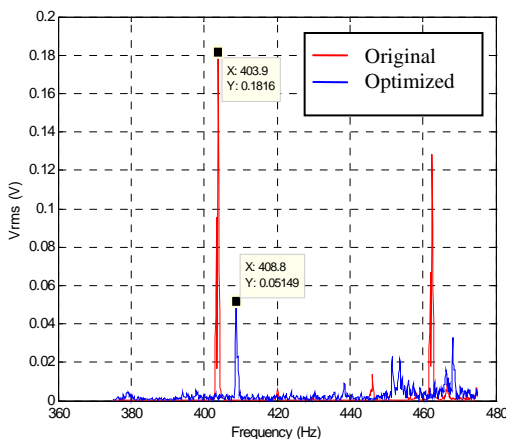


Fig. 7. Vibration analysis

The differences between the simulated and practical results are related to the ferromagnetic material characteristic used in the simulation, which does not represent accurately the real one, the tolerances in the

geometric design, and the inaccuracy in the measurements and drive position angles adjusting.

The SRM phase A current, voltage, and the rotor frequency pulse waveforms for each rotor/motor test are depicted in Figures 8 and 9. In both cases, the voltage signal was measured with channel (Ch2) in inverted mode. The Ch1 voltage scale is 100 mV / Amp, while the Ch2 voltage scale is 100 V / div.

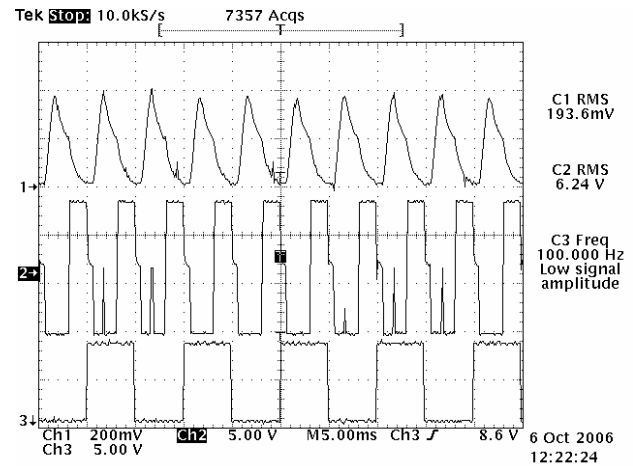


Fig. 8. Original Rotor Signals Measurement (Ch1- Phase A current, Ch2 – Phase A Inverter Voltage and Ch3 – Rotor Speed Signal)

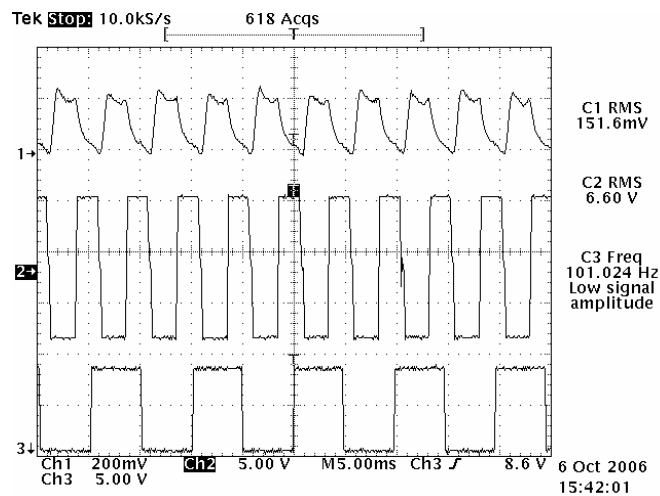


Fig. 9. Optimized Rotor Signals Measurement (Ch1- Phase A current, Ch2 – Phase A Inverter Voltage and Ch3 – Rotor Speed Signal)

Comparing the two current waveform profiles obtained, it can be observed that the optimized rotor current waveform is “flatter” than the original one. This difference between both current waveform profiles is related to the changes implemented in the optimized rotor geometric parameters, which implied in different torque ripple profiles.

## VIII – CONCLUSIONS

In spite of the crescent technological development and the existence of countless simulation tools to aid in

machines projects, a higher precision in SRM's parameters only can be obtained by experimental tests.

In order to minimize the torque ripple and increase its starting torque in the special SRM, it was established an optimization procedure that uses the FEM, Simulated Annealing (SA) and Kriging Method to determine the values of the three geometric parameters:  $\beta_0$ ,  $l_{g1}$  and  $l_{g2}$ , chosen as the most significant parameters. The results of the torque ripple obtained in the simulations show a reduction of 44% in the optimized prototype, considering the original design as the reference.

After the numerical optimization, prototypes were manufactured and tested. To test the prototypes it was used the vibration data to determine the comparatives values of torque ripple.

Despite some discrepancies, the results show that the optimization reached the proposed aim. Considering the original design as the reference, the optimized prototype presents a 72.65% smaller torque ripple.

#### ACKNOWLEDGEMENTS

The authors acknowledge J. Sanches for technical support in the vibration tests, J. F. R Mello. for the technical support in the power drive assembling, A. Mathiazzi and F. Duarte for help with the torque and vibration measurements, L. Buzo for the figures edition, A. Tosin for helping us with the technical and grammar English review and finally the support of the CTMSP.

#### REFERENCES

- [1] Pillay P., Cai W., Tang Z., Omeckanda A., Vibration Measurements in the Switched Reluctance Motor – IEEE 2001;
- [2] Pillay P., W. Cai, "An investigation into vibration in the switched reluctance motor," IEEE Transactions on Industrial Applications, Vol. 35, No.3, May/June 1999, pp. 589~596.
- [3] I.E. Chabu; S.I. Nabeta; J.R. Cardoso. "Design Aspects Of 4:2 Pole-2 Phase Switched Reluctance Motors", Proceedings of the IEEE-IEMDC'99, v. 1, p. 63-65, 1999;
- [4] S.I. Nabeta, D.A.P. Correa, W.M. da Silva, et al.: Mitigation of the Torque Ripple of a Switched Reluctance Motor Through a Multi-Objective Optimization. 16th International Conference on the Computation of Electromagnetic Fields, p.827-828 Compumag 2007,
- [5] S.I. Nabeta, I. E.Chabu, L. Lebensztajn et al.: Kriging Models and Torque Improvements of a Special Switched Reluctance Motor. International Electric Machines and Drives Conference, IEMDC 2007, p. 559-563
- [6] L. Lebensztajn et al.; "Kriging: a useful tool to electromagnetic devices optimization". IEEE Trans. on Mag., v. 40, n. 2, pp. 1196-1199, 2004.
- [7] T.J.E. Miller, "Electronic Control of Switched Reluctance Machines", Newness Power Engineering Series, 2001;
- [8] R. Krishnan, "Switched Reluctance Motor Drives". CRC Press, 2001.
- [9] Matlab. Mathworks Software release 14.